X-Architecture Steiner Minimal Tree Construction Based on Discrete Differential Evolution

Hailin Wu[1], Saijuan Xu[2], Zhen Zhuang[1,3], and Genggeng Liu[1,3(✉)]

[1] College of Mathematics and Computer Sciences, Fuzhou University, Fuzhou 350116, China
15505915786@163.com, zhuang_zhen@126.com, liugenggeng@fzu.edu.cn

[2] Department of Information Engineering, Fujian Business University, Fuzhou 350012, China
l044513210@qq.com

[3] Fujian Provincial Key Laboratory of Network Computing and Intelligent Information Processing, Fuzhou University, Fuzhou 350116, China

Abstract. As the best connection model for the multi-pin net of the non-Manhattan architecture global routing problem, the X-architecture Steiner Minimum Tree (XSMT) construction is a Non-deterministic Polynomial hard (NP-hard) problem. The Differential Evolution (DE) algorithm has shown good application effect in solving various NP-hard problems. For this reason, based on the idea of DE algorithm, this paper proposes an XSMT construction algorithm for solving this problem. First of all, because the traditional DE algorithm is designed for continuous problems, the optimization ability is limited in solving discrete problems. This paper proposes a novel crossover operator and mutation operator. At the same time, in order to maintain the effectiveness of the evolutionary algorithm, an Edge-to-Point coding strategy suitable for evolutionary algorithms is proposed to better preserve the optimal substructure of the population. Finally, in order to speed up the convergence speed and quality of the algorithm, this paper proposes an initial solution based on the minimum tree generation algorithm. Experiments show that the effectiveness of the proposed algorithm and related strategies can construct a high-quality XSMT solution.

Keywords: XSMT · Routing · VLSI · Steiner minimal tree · Different evolution

1 Introduction

Global routing is an important part of Very Large Scale Integration (VLSI) physical design. Steiner Minimal Tree (SMT) problem is to find a minimum connection tree for a given pin set by introducing some additional Steiner points. SMT problem is a Non-deterministic Polynomial hard (NP–hard) problem [1]. SMT model is the best connection model for VLSI global routing [2, 3]. How to construct a suitable SMT is a problem that needs to be solved in VLSI manufacturing process.

Y. Liu et al. (Eds.): ICNC-FSKD 2019, AISC 1074, pp. 433–442, 2020.
https://doi.org/10.1007/978-3-030-32456-8_47

At present, most of the existing algorithms for solving global routing problem are based on the Manhattan architecture [4–6]. With the development of VLSI fabrication technology, the optimization capacity of routing algorithms based on the Manhattan architecture is limited. It is gradually becoming the major challenges of chip performance. Based on this background, more and more researchers begin to study the non-Manhattan architecture which can use much more routing resources to better optimize wirelength.

The primary research work for non-Manhattan architecture routing is to construct a SMT based on non-Manhattan architecture. X-Architecture Steiner Minimal Tree (XSMT) is the representative architecture of non-Manhattan architecture routing [7–12]. SMT problem is a NP-hard problem. Meanwhile, evolutionary algorithm has shown good application effect in solving various NP-hard problems. So researchers began to study the application of evolutionary algorithm in SMT construction.

As a kind of swarm-based heuristic search algorithm, Differential Evolution (DE) algorithm was first proposed in 1995 [13]. DE is a kind of evolutionary algorithm and used to solve real number optimization problems. Compared with other optimization algorithms, DE algorithm has many characteristics such as undetermined parameters, simple structure, easy implementation, fast convergence and strong robustness. It is widely used in various fields such as pattern recognition, artificial neural network and so on [14–19].

Based on the above research work, this paper proposes an XSMT construction algorithm based on Discrete DE algorithm (XSMT-DDE). Firstly, in order to speed up the convergence speed and quality of the algorithm, this paper proposes an initial solution based on the minimum spanning tree algorithm. Secondly, according to the characteristics of XSMT, this paper proposes a discrete DE update strategy combined with the crossover operator and the mutation operator. And thus the proposed algorithm can be used for XSMT construction problem. Finally, the experimental testcases are carried out and they show the feasibility and effectiveness of the proposed algorithm.

2 Problem Description

The given set $P = \{P_1, P_2, \cdots, P_n\}$ in the XSMT problem is a set of n pins to be routed. The Cartesian coordinate system is introduced, and each P_i corresponds to one coordinate (x_i, y_i), For example, Table 1 shows that there are 5 pins in the net to be routed. The input information of the given pins is shown in the Table 1. The corresponding pin distribution is shown in Fig. 1. For example, the pin 1 is shown in the second column of Table 1, and the value of point 1 is $(21, 2)$.

Table 1. The input information of the given pins

N	1	2	3	4	5
X	21	3	10	23	15
Y	2	4	5	12	23

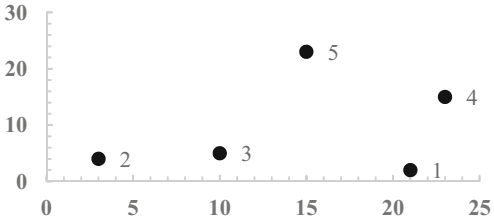

Fig. 1. The pin distribution for a given net in Table 1.

Definition 1 Pseudo-Steiner. For convenience, we assumes that the connection point except for the pins is called Pseudo-Steiner point, which is denoted as point *S*.

Definition 2 (Choice 0). As shown in Fig. 2a, let $A = (x_1, y_1)$ and $B = (x_2, y_2)$ be the two endpoints of segment $\overline{AB}$, where $x_1 < x_2$. The Choice 0 of $\overline{AB}$ leads rectilinear edge from A to S, and then leads octagonal edge from S to B.

Definition 3 (Choice 1). As shown in Fig. 2b, it leads octagonal edge from A to S, and then leads rectilinear egde from S to B,.

Definition 4 (Choice 2). As shown in Fig. 2c, it leads vertical edge from A to S, and then leads horizontal edge from S to B.

Definition 5 (Choice 3). As shown in Fig. 2d, it leads horizontal edge to S, and then leads vertical edge from S to B.

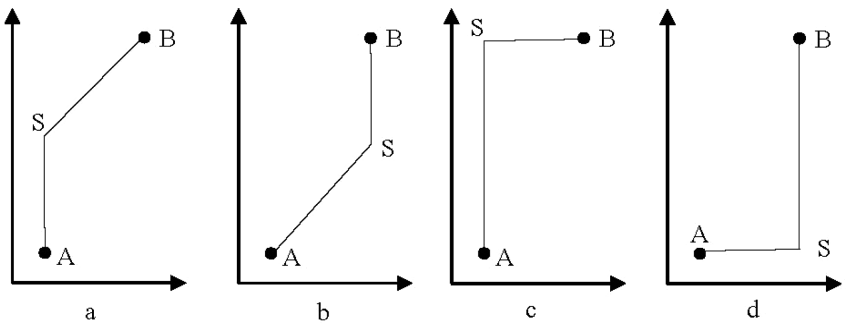

Fig. 2. Four choice of segment $\overline{AB}$

3 DE Algorithm

The essence of DE is an efficient multi-objective global optimization algorithm. It is used to solve global optimal solution in multidimensional space. Through continuous differential evolution, it can get the optimal solution.

3.1 Process of Traditional DE Algorithm

According to Literature [13], the flow chart of traditional differential evolution algorithm is as follows.

Step1: Population initialization N particles are randomly generated in the solution space, each of which has an m-dimensional vector composition, and the j-dimensional vector of the *i-th* particle is denoted as follow.

$$X_i^j = L_{j\_min} + rand(0,1) * \left(L_{j\_max} - L_{j\_min}\right) \tag{1}$$

where L_{j_min} and L_{j_man} are the maximum value and the minimum value of dimension j respectively.
Step2: Mutation During the *g-th* iteration, the mutation strategy is denoted as follow.

$$V_i(g) = X_{p1}(g) + F * \left(X_{p2}(g) - X_{p3}(g)\right) \tag{2}$$

where $p_1 \neq p_2 \neq p_3 \neq i$, F is the scaling factor and is selected between [0, 2].
Step3: Crossover The crossover strategy of DE algorithm is denoted as follow.

$$v_i^j = \begin{cases} h_i^j(g) & rand(0,1) \leq cr \\ x_i^j(g) & else \end{cases} \tag{3}$$

where cr is a cross probabilistic, and $cr \in [0, 1]$.
Step4: Selection The selection strategy is a greedy strategy. It is denoted as follow.

$$X_i(\mathrm{g}+1) = \begin{cases} V_i(g) & f(V_i(g)) < f(X_i(g)) \\ X_i(g) & else \end{cases} \tag{4}$$

Step5: If the algorithm termination condition is met, it ends. Otherwise, it returns **Step2**.

4 XSMT-DDE Algorithm

4.1 Coding Strategy

Generally, there are two encoding strategies of spanning trees, including Prufer number coding and Edge-to-Point coding. Because the Edge-to-Point coding strategy is more suitable for evolution algorithm, we use the Edge-to-Point coding strategy. The Edge-to-Point coding strategy is defined as below. If a net has n pins, a spanning tree would have *n–1* egdes, *n–1* Pseudo Steiner points and one extra bit which is the particle's fitness. For example, the spanning tree which is give in Fig. 1 can be expressed as the following numeric string.

1 3 0 2 3 1 3 5 2 4 5 2 23

where the number '23' is the fitness of the particle and it is also the length of the spanning tree.

4.2 The Fitness Function of the Particle

The length of an XSMT is the sum of the length of all the edge in the tree. The length of an XSMT is defined as below.

$$L(T_x) = \sum\nolimits_{e_i \in T_x} l(e_i) \tag{5}$$

where $l(e_i)$ represents the length of edge e_i in XSMT.

To measure the cost of an XSMT in our algorithm, the smaller the total length of the XSMT, the higher its cost is. In this paper, the fitness function which is used to measure the cost of an XSMT is defined as below.

$$f = \frac{1}{L(T_x) + 1} \tag{6}$$

When the pins of a routing tree are coincided, it causes that the length of the routing tree is 0 which means the denominator is meaningless. In order to avoid the happening of this problem, we add one to the denominator.

4.3 Particle Updating Formula

DE algorithm is a type of multi-objective optimization algorithms. It is used to get global optimal solution for continuous problem. However, XSMT problem is a discrete problem. It cannot be solved directly by DE algorithm. In order to solve this problem, this paper proposes a novel crossover operator and a novel mutation operator.

Novel Mutation Operator: Combining with the mutation strategy of formula (2), it is defined as below. Let F is equal to 1, the subtraction operation in the formula refers to the difference set operation, and the addition operation refers to the union operation of the set. For this improvement, the subtraction operation may produce two results as below.

A. As shown in Fig. 3, three selected particles $p1$, $p2$ and $p3$ are substituted into formula (2), and the result of $p2 - p3$ is empty set. Then the particle $p1$ selects an edge $m1$ which is randomly deleted to mutate. After deletion, $p1$ is divided into two sub trees. Combining with Disjoint Set Union (DSU), two points are randomly selected from the two sub trees respectively and reconnected as a mutation particle.
B. As shown in Fig. 4, according to formula (2), the result of $p2 - p3$ is not empty. Combining with DSU, the elements of the difference set are as part of the edge set of mutation result. Then we select the remaining from the edge set of the particle $p1$ to reconstruct a new tree as a mutation particle.

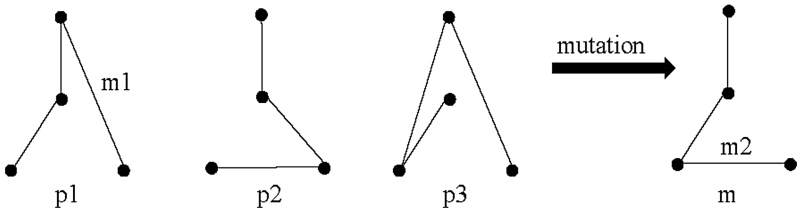

Fig. 3. Novel mutation operator 1

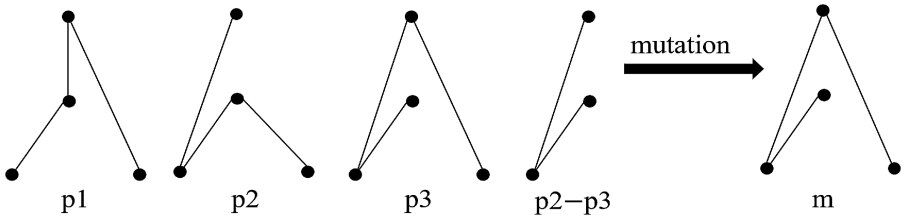

Fig. 4. Novel mutation operator 2

Novel Crossover Operator: The object to be crossed are two trees. If the formula (3) is used directly, the result of the crossover may be an illegal tree. To solve this problem, the following improvements are proposed. We cross the mutation particle with the current particle, and it is performed according to the probability *cr*. As shown in Fig. 5, after the mutation operation, the mutated particle *m* cross with the current particle *i*. The common edges of the two trees are used as the starting set, and the remaining edges are used as the candidate edges. Combining with DSU, we constantly extract the remaining edges from the candidate edges until the crossover result is a legal tree.

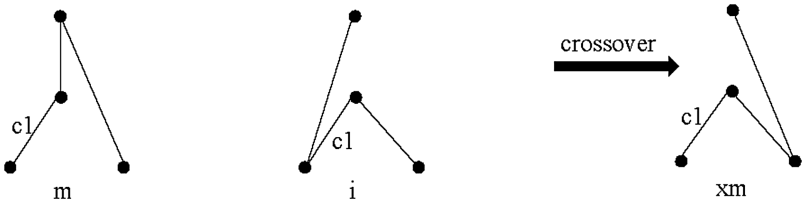

Fig. 5. Novel crossover operator

Selection Operator: The selection operator is based on formula (4).

4.4 Algorithm Flow of This Paper

The flow chart of the XSMT-DDE algorithm is shown in Fig. 6. The detailed steps are as below.

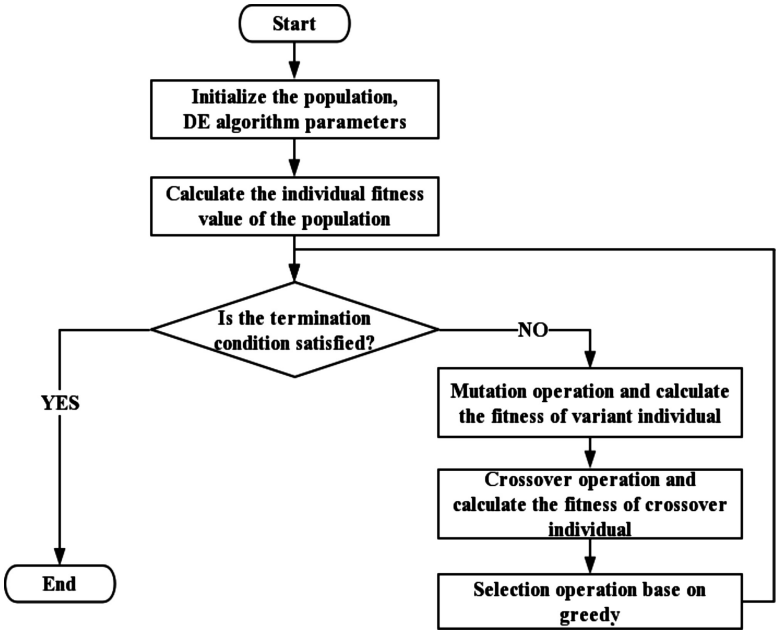

Fig. 6. The flow chart of the proposed algorithm

Firstly, read the pin information of the routing to be tested, and sort the pin coordinates in ascending order.

Secondly, the population is initialized by the minimum spanning tree method and the fitness value is calculated according to formula (6). Then set the number of iterations, the scaling factor F and the crossover probability cr.

Thirdly, in each iteration process, the particle population is updated by the mutation operator, crossover operator and selection strategy proposed in this paper, and the fitness value is calculated according to formula (6).

Finally, if the algorithm termination condition is met, it ends, otherwise, it returns to the third step.

5 Experimental Results

The algorithm in this paper is written in C/C++ language and implemented on Windows10 platform. The test routing data used to verify the validity of the algorithm comes from the literature [10]. In order to verify that the proposed algorithm can solve the XSMT problem, the algorithm is compared with the literature [4, 10]. The experimental results are given in the following sections.

5.1 Parameter Setting Relating to Algorithm

The main parameter setting of the XSMT-DDE algorithm includes the population size *NP*, the number of iterations, the scaling variable *F* and the crossover probability *cr*. In our implement, *F* is equal to 1 and *cr* adopts an adaptive strategy which is defined as below.

$$cr_i = \begin{cases} cr_l + (cr_u - cr_l)\frac{f_i - f_{min}}{f_{max} - f_{min}} & f_i > \overline{f} \\ cr_l & else \end{cases} \tag{7}$$

where cr_l is equal to 0.1 and cr_u is equal to 0.6.

5.2 Verify the Validity of the Minimum Tree Generation Method

In this paper, the population is generated by the minimum spanning tree method which avoids the situation that the algorithm solution space is too large to be converged due to random initialization. The specific experimental results are shown in Table 2. The last column is reduction rates. It can be seen from the last column in the Table 2 that, as the number of pins of basic circuits increases, the minimum spanning tree method can effectively optimize the situation to get over that the algorithm cannot converge due to the large solution space. It achieves an average optimization 35.72%.

Table 2. Optimization rate brought by minimum tree generation strategy

Test	Pins	Random initial solution	Minimum spanning tree	Reduction (%)
1	8	16900	16900	0.00%
2	9	18023	18023	0.00%
3	10	19397	19397	0.00%
4	20	32219	32198	0.07%
5	50	55751	47932	14.02%
6	70	80640	56347	30.13%
7	100	123767	68855	44.37%
8	410	1042081	141666	86.41%
9	500	1378707	154697	88.78%
10	1000	3388682	221739	93.46%
Average				35.72%

5.3 Comparison with Other Algorithms

In order to verify the effectiveness of the proposed algorithm, the results of our algorithm are compared with the results of the literature [4, 10]. The experimental results are shown in Table 3. The experimental results show that the XSMT-DDE algorithm achieves an optimization rate of 9.61% and 0.37% in solving the XSMT problem compared with the traditional strategies of Rectilinear Steiner Minimal Tree (RSMT)[4] and Octagonal Steiner Minimal Tree (OSMT) [10]. This algorithm can solve the XSMT construction problem better.

Table 3. Comparison between XSMT-DDE and other algorithms

Test	Pins	RSMT (R)	OSMT	XSMT-DDE	Reduction (%)	
					XSMT-DDE:RSMT	XSMT-DDE:OSMT
1	8	17931	17040	16900	5.75%	0.82%
2	9	20503	18163	18023	12.10%	0.77%
3	10	21910	19818	19397	11.47%	2.12%
4	20	35723	32199	32198	9.87%	0.00%
5	50	53383	47960	47932	10.21%	0.06%
6	70	61987	55980	56347	9.10%	−0.66%
7	100	76016	68743	68855	9.42%	−0.16%
8	410	156520	142880	141666	9.49%	0.85%
9	500	170273	154290	154697	9.15%	−0.26%
10	1000	245201	222050	221739	9.57%	0.14%
Average					9.61%	0.37%

6 Conclusion

In this paper, we apply an improved DE algorithm to solve VLSI routing problem. Compared to traditional DE algorithms which are used to solve continuous problems, our algorithm can be effectively used to solve discrete problems by adopting some improved strategies so that it can solve the problem of constructing XSMT. The experiment results show that our algorithm is effective to construct XSMT.

Acknowledgements. This work was partially supported by the National Natural Science Foundation of China (Nos. 61877010 and 11501114), and the Fujian Natural Science Funds (No.2019J01243).

References

1. Garey, M.R., Johnson, D.S.: The rectilinear Steiner tree problem is NP-complete. SIAM J. Appl. Math. **32**(4), 826–834 (1977)
2. Lavagno, L., Markov, I.L., Martin, G., et al.: Electronic Design Automation for IC Implementation, Circuit Design, and Process Technology: Circuit Design, and Process Technology. CRC Press, Boca Raton (2016)
3. Stroud, C.E., Wang, L.T., Chang, Y.W.: Chapter 1: Introduction. In: Ang, L.T., Chang, Y. W., Cheng, K.T., Electronic Design Automation: Synthesis, Verification, and Testing, pp. 1–38, Elsevier/Morgan Kaufmann (2009)
4. Liu, G.G., Chen, G.L., Guo, W.Z., et al.: DPSO-based rectilinear Steiner minimal tree construction considering bend reduction. In: Proceeding of the 7th International Conference on Natural Computation, pp. 1161–1165 (2011)
5. Held, S., Muller, D., Rotter, D., et al.: Global routing with timing constraints. IEEE Trans. Comput. Aided Des. Integrated Circuits Syst. **37**(2), 406–419 (2018)
6. Siddiqi, U.F., Sait, S.M.: a game theory based post-processing method to enhance VLSI global routers. IEEE Access **5**, 1328–1339 (2017)

7. Coulston, C.S.: Constructing exact octagonal steiner minimal trees. In: Proceedings of the 13th ACM Great Lakes symposium on VLSI, pp. 1–6. ACM (2003)
8. Chiang, C., Chiang, C.S.: Octilinear Steiner tree construction. In: The 2002 45th Midwest Symposium on Circuits and Systems, vol. 1, pp. 1–603 (2002)
9. Zhu, Q., Zhou, H., Jing, T., et al.: Spanning graph-based nonrectilinear steiner tree algorithms. IEEE Trans. Comput. Aided Des. Integrated Circuits Syst. **24**(7), 1066–1075 (2006)
10. Liu, G.G., Chen, G.L., Guo, W.Z.: DPSO based octagonal steiner tree algorithm for VLSI routing. In: Proceeding of the 5th International Conference on Advanced Computational Intelligence (ICACI2012), pp. 383–387 (2012)
11. Liu, G.G., Huang, X., Guo, W.Z., et al.: Multilayer obstacle-avoiding X-architecture Steiner minimal tree construction based on particle swarm optimization. IEEE Trans. Cybern. **45**(5), 989–1002 (2015)
12. Liu, G.G., Guo, W.Z., Niu, Y.Z., et al.: A PSO-based timing-driven Octilinear Steiner tree algorithm for VLSI routing considering bend reduction. Soft. Comput. **19**(5), 1153–1169 (2015)
13. Storn, R., Price, K.: Differential evolution – a simple and efficient heuristic for global optimization over continuous spaces. J. Global Optim. **11**(4), 341–359 (1997)
14. Zhou, Y.Z., Yi, W.C., Gao, L., et al.: Adaptive differential evolution with sorting crossover rate for continuous optimization problems. IEEE Trans. Cybern. **47**(9), 2742–2753 (2017)
15. Qiu, X., Xu, J.X., Xu, Y., et al.: A new differential evolution algorithm for minimax optimization in robust design. IEEE Trans. Cybern. **48**(5), 1355–1368 (2018)
16. Yong, W., Hao, L., Long, H., et al.: Differential evolution with a new encoding mechanism for optimizing wind farm layout. IEEE Trans. Ind. Inf. **14**(3), 1040–1054 (2018)
17. Ge, Y.F., Yu, W.J., Lin, Y., et al.: Distributed differential evolution based on adaptive mergence and split for large-scale optimization. IEEE Trans. Cybern. **48**(7), 2166–2180 (2018)
18. Zhou, X.G., Zhang, G.J.: Differential evolution with underestimation-based multimutation strategy. IEEE Trans. Cybern. **49**(4), 1353–1364 (2019)
19. Wang, J., Liang, G., Zhang, J.: Cooperative differential evolution framework for constrained multiobjective optimization. IEEE Trans. Cybern. **49**(6), 2060–2072 (2018)

Detection Models Study of Chlorophyll in Winter Wheat's Leaves by Reflectance Spectra and Artificial Neural Networks

Zhenhong Rao[1(✉)], Li Zhang[1], and Xue Liang[2]

[1] College of Science, China Agricultural University, Beijing 100083, China
ndrzh@sina.com
[2] College of Information and Electrical Engineering, China Agricultural University, Beijing 100083, China

Abstract. Reflectance spectra of living wheat's leaves were acquired by portable radiation spectrometer. Multivariate scatter correction (MSC) method was used to preprocess the spectra, and quantitative analysis detection models were built up by artificial neural networks (ANN). The models of chlorophyll, chlorophyll a, and chlorophyll b in leaves were built up and tested. In calibration set and predicted set, for chlorophyll in leaves, the correlation coefficient (R) were 0.927 and 0.818, the standard deviation (SD) were 0.252 and 0.470; for chlorophyll a in leaves, the correlation coefficient (R) were 0.780 and 0.627, the standard deviation (SD) were 0.441 and 0.592; for chlorophyll b in leaves, the correlation coefficient (R) were 0.876 and 0.871, the standard deviation (SD) were 0.205 and 0.259. The results show that, using portable radiation spectrometer to acquire the reflectance spectra, multivariate scatter correction to preprocess the spectra, and artificial neural networks to build up the models, the chlorophyll, chlorophyll a and chlorophyll b in winter wheat's leaves may be quantitative detected.

Keywords: Artificial neural networks · Spectral analysis · Winter wheat's leaves · Chlorophyll · Chlorophyll a · Chlorophyll b

1 Introduction

The measurement and diagnosis of chlorophyll, chlorophyll a and chlorophyll b in winter wheat plants are important links in the production process of winter wheat. The conventional technique for the diagnosis of winter wheat nutrients is destructive sampling and its analysis time is longer. This sampling analysis technique is difficult to meet the requirements of modern agriculture for water and nutrient management. Although portable instruments can measure the SPAD (Soil and Plant Analyzer development) value, which has relation with chlorophyll, but the content of chlorophyll a and chlorophyll b cannot be measured. Retrieving the biochemical components of crops with crop spectral information has the advantages of timely, rapid, non-invasive sampling, so spectral analysis techniques are ideal techniques for the diagnosis of crop nutrient conditions [1–3].

Y. Liu et al. (Eds.): ICNC-FSKD 2019, AISC 1074, pp. 443–451, 2020.
https://doi.org/10.1007/978-3-030-32456-8_48

Multivariate scatter correction (MSC) and artificial neural network (ANN) are methods that have been used more actively in crop spectra processing in recent years. It is mostly used for the detection of biochemical components such as oils, proteins, starches, fatty acids, etc. which in cereals, seeds, dried leaves (tobacco), powders, etc. MSC was used as preprocess method [4, 5] and ANN was used as to build quantitative analysis models [6–9]. ANN was also used to estimation of rice pigment content [10] and estimation of sugar to nitrogen ratio in wheat leaves [11].

In this paper, the reflectance spectra of living winter wheat leaves were acquired by portable radiation spectrometer. The acquired spectra were pretreated by multivariate scatter correction pretreatment method. Standard chlorophyll value and preprocessed spectral data were used by artificial neural network (ANN) to establish a quantitative analysis model, aiming at establishing a model with high prediction accuracy, studying the spectrum detection mechanism of winter wheat biochemical components, and achieving the goal of directly predicting the content of chlorophyll, chlorophyll a and chlorophyll b in winter wheat leaves by spectral information.

2 Experiment

2.1 Acquisition of Winter Wheat Leaf Reflection Spectra

Select 40 winter wheat plants, cut the second leave of each plant, wipe off the surface dirt for use. The reflectance spectra of the 40 winter wheat leaves were scanned by using the FieldSpec® Pro FR portable spectroradiometer from the US ASD and the 1800 integrating sphere produced by LI-COR. The spectral range is 400 nm to 1550 nm, the data are collected in each nanometer of the spectral region. The absorption of chlorophyll is in the visible region, so the spectral range of 400–750 nm was selected to study. The front of the wheat leave was placed in front of the aperture, and the reference plate and the wheat leaves were separately measured. Each leave was scanned 5 times and averaged to reduce the error. The measured reflectance spectrum is shown in Fig. 1.

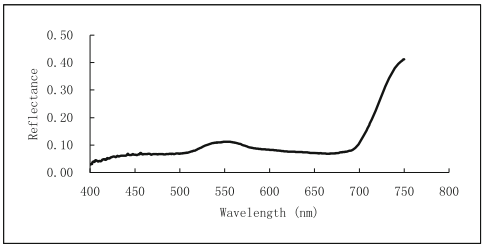

Fig. 1. Reflection spectrum of winter wheat leaves

2.2 Determination of Standard Value of Leaf Chlorophyll Content

After spectral scanning, the chlorophyll, chlorophyll a, and chlorophyll b contents in the leaves were measured by standard methods and used as the standard chemical values of the leaves to build quantitative models by artificial neural networks.

The standard methods is as following: After the leaves are ground and extracted, the absorbance values of the extracts at 663 nm and 645 nm were measured on a spectrophotometer, and the concentrations of chlorophyll, chlorophyll a and chlorophyll b in the solution were calculated by substituting A-M equation.

$$\text{Chlorophyll a concentration}: \quad C_{\mathrm{a}} = 12.7A_{663} - 2.69A_{645} \tag{1}$$

$$\text{Chlorophyll b concentration}: \quad C_{\mathrm{b}} = 22.9A_{663} - 4.68A_{645} \tag{2}$$

$$\text{Chlorophyll concentration}: \quad C_T = 8.02A_{663} + 20.12A_{645} \tag{3}$$

Among them, A_{645} and A_{663} are the absorbance values of chlorophyll extract at monochromatic light at wavelengths of 645 and 663 nm, respectively, and the unit of chlorophyll content is mg/g.

The chlorophyll a, chlorophyll b, and total chlorophyll content were calculated according to the following formula.

$$\text{Chlorophyll a content}\,(\text{mg/g}) = \frac{C_{\mathrm{a}} \times W_{\mathrm{t}}}{W_Y \times 1000} \tag{4}$$

$$\text{Chlorophyll b content}\,(\text{mg/g}) = \frac{C_{\mathrm{b}} \times W_{\mathrm{t}}}{W_Y \times 1000} \tag{5}$$

$$\text{Total chlorophyll content}\,(\text{mg/g}) = \frac{C_{\mathrm{T}} \times W_t}{W_Y \times 1000} \tag{6}$$

Where W_t is the total amount of extract (ml), W_Y is fresh weight (g) for the sample.

It was determined that the highest chlorophyll content in the 40 winter wheat leaves was 4.980 mg/g, the lowest value was 2.021 mg/g, and the average value was 2.873 mg/g. The highest chlorophyll a content was 2.809 mg/g, the lowest value was 0.826 mg/g, and the mean value was 1.364 mg/g; The highest chlorophyll b content was 2.476 mg/g, the lowest value was 0.606 mg/g, and the mean was 1.509 mg/g.

3 MSC Pretreatment of Winter Wheat Reflectance Spectra

The acquired reflection spectrum of winter wheat leaves was pretreated by multivariate scattering correction method. The Algorithm of MSC is as following: Usually calculate the average spectrum of all the samples as the standard spectrum, operate each sample spectrum with the method of unary linear regression to get their regression constant and regression coefficients, and then correct the original spectra of each sample to improve the signal-to-noise ratio.

Multivariate scattering correction eliminates the influence of environmental factors on spectral information, separates the effects of scattering from the original spectrum, and enhances the spectral information associated with the content of the component to be tested. Thereby increasing the signal to noise ratio of the spectrum. The acquired reflection spectrum of winter wheat leaves was pretreated by multivariate scattering correction method to eliminate the influence of scattering.

4 The Structure of ANN

A back-propagation neural network was constructed by using three layers of nodes: an input layer, a hidden layer, and an output layer, as shown in Fig. 2.

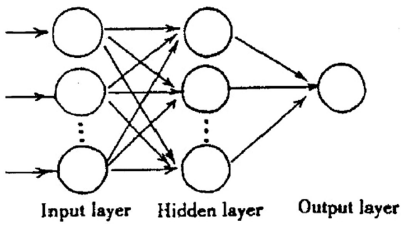

Fig. 2. Three layers B-P ANN for chlorophyll content in winter wheat leaves

Artificial neural network is a nonlinear modeling method that can establish a nonlinear model between input parameters and output parameters. The advantage is that the established model is stable and the relative error is small. The ANN consists of an input layer, a hidden layer, and an output layer. In the spectral analysis, the characteristic parameter of the spectrum is taken as the node value of the input layer, and the sample content value to be obtained is used as the node value of the output layer. In this paper, the node value of the input layer of ANN is the principal component of the spectrum, and the node value of the output layer is the value of chlorophyll (chlorophyll a, chlorophyll b) to be obtained.

5 Establishment of Spectral Detection Model for Chlorophyll Content in Winter Wheat Leaves

The reflection spectrum of winter wheat leaves was pretreated by multivariate scattering correction method, and then the principal components of the spectrum were calculated. The number of suitable principal components is determined by comprehensively comparing the prediction results. The extracted principal component is used as the input of the neural network to establish a quantitative analysis test model of the artificial neural network.

The sample is divided into two parts: the calibration set and the predicted set. The calibration set contains 30 samples for establishing a calibration model for quantitative

analysis. There are 10 samples in the predicted set to test the applicability of the model. The optimal principal component number is calculated.

In Matlab, newff is used to create a network. For estimation chlorophyll, the parameters of neural network model are as follows:

net.trainParam.lr = 0.1; % the learning rate of training is set to 0.1.
net.trainParam.mc = 0.1; % the momentum coefficient is set to 0.1.
net.trainParam.epochs = 20; % the training epochs is set to 20.
net.trainParam.goal = 0.08; % the error of training objective is set to 0.08.

For estimation chlorophyll a and chlorophyll b, the four parameters of neural network model are set as 0.1, 0.1, 20, 0.3.

After much training, a model with better prediction results is obtained. The calibration set data was modeled. Table 1 shows the optimal principal component number, as well as correlation coefficient (R) and standard deviation (SD) between chemical values and predicted values in the calibration set and predicted set. Figures 3 and 4 is a plot of the predicted and chemical values of chlorophyll in winter wheat leaves in calibration set and predicted set respectively. Figures 5 and 6 is a plot of chlorophyll a. Figures 7 and 8 is a plot of chlorophyll b.

Table 1. The results of calibration and predicted set for ingredients

Ingredient	PC number	Calibration set	Predicted set
Chlorophyll	5	R = 0.927 SD = 0.252	R = 0.818 SD = 0.470
Chlorophyll a	3	R = 0.780 SD = 0.441	R = 0.627 SD = 0.592
Chlorophyll b	4	R = 0.876 SD = 0.205	R = 0.871 SD = 0.259

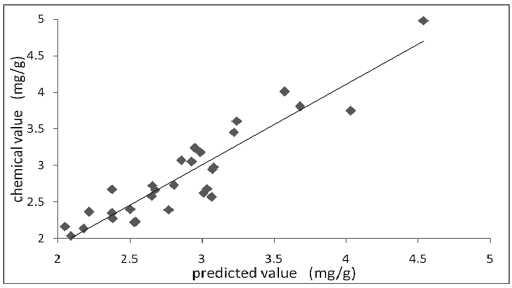

Fig. 3. Relationship between predicted and chemical values of chlorophyll content in winter wheat leaves in the calibration set

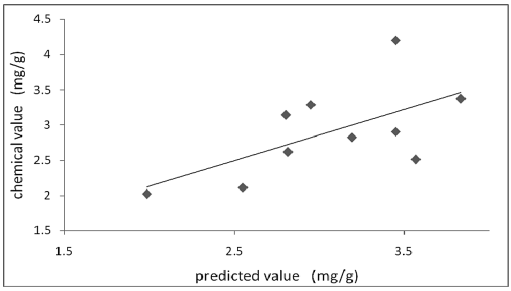

Fig. 4. Relationship between predicted and chemical values of chlorophyll content in winter wheat leaves in the predicted set

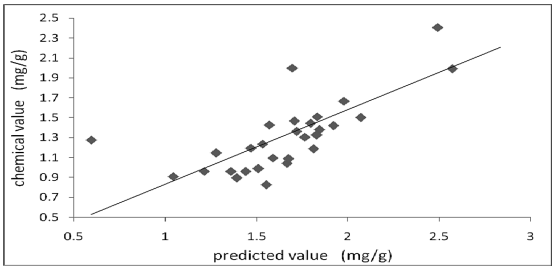

Fig. 5. Relationship between predicted and chemical values of chlorophyll a content in winter wheat leaves in the calibration set

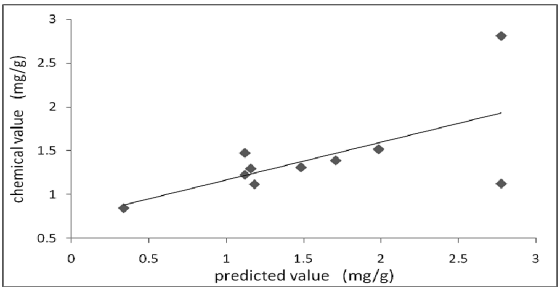

Fig. 6. Relationship between predicted and chemical values of chlorophyll a content in winter wheat leaves in the predicted set

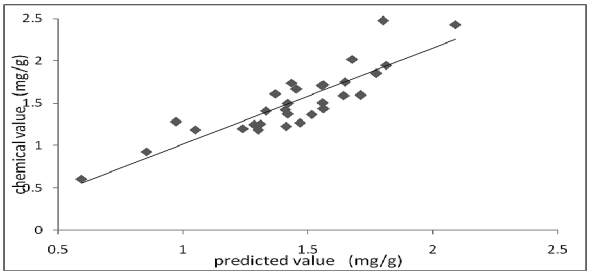

Fig. 7. Relationship between predicted and chemical values of chlorophyll b content in winter wheat leaves in the calibration set

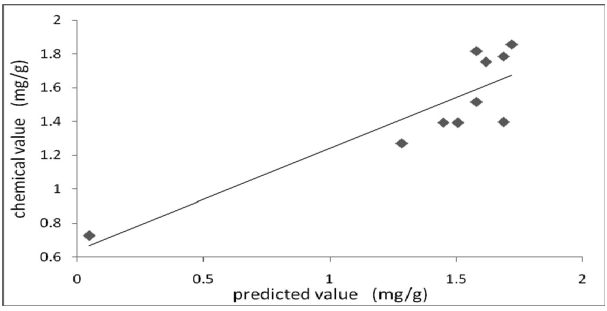

Fig. 8. Relationship between predicted and chemical values of chlorophyll b content in winter wheat leaves in the predicted set

6 Discussion

The spectral data of the wild winter wheat leaves are acquired. The scattering caused by the external environmental factors will cause the collected spectral data to contain invalid information. Therefore, the spectral data is preprocessed by the multivariate scatter correction method, and the scatter correction is obtained. Spectral data after scatter correction can effectively eliminate the effects of scattering and enhance the spectral information associated with the component content. The back propagation artificial neural network is a powerful learning system that can achieve a highly nonlinear mapping between input and output. After multiple learning and training, a predictive model with better predictability can be obtained.

The error mainly comes from two aspects. One is that when measuring the reflection spectrum, the placement position of the wheat leave has certain influence on the spectrum measurement. The other is the errors caused in the measurement of the chlorophyll, chlorophyll a and chlorophyll b by laboratory method, that is the degree of chlorophyll extraction in leaves has a certain effect on the measurement of chlorophyll content in leaves.

7 Results and Conclusion

In this paper, the reflectance spectra of winter wheat leaves were acquired by portable radiation spectrometer. The spectra were preprocessing by multivariate scatter correction. The quantitative analysis model of chlorophyll, chlorophyll a and chlorophyll b in leaves was established by artificial neural network method. The correlation coefficients of modeling and test for chlorophyll in leaves were 0.927 and 0.818 respectively; the standard deviations of modeling and test were 0.252 and 0.470 respectively. The correlation coefficients of modeling and test for chlorophyll a in leaves were 0.780 and 0.627 respectively; the standard deviations of modeling and test were 0.441 and 0.592 respectively. The correlation coefficients of modeling and test for chlorophyll b in leaves were 0.876 and 0.871 respectively; the standard deviations of modeling and test were 0.205 and 0.259 respectively.

In summary, the reflectance spectra of winter wheat leaves were acquired by portable radiation spectrometer. The multivariate scatter correction pretreatment of the spectra was carried out. The quantitative analysis model of artificial neural network was established to quantitatively analyze the chlorophyll, chlorophyll a and chlorophyll b in winter wheat leaves. The results are satisfactory. This method can be used in agricultural practice.

Acknowledgements. The authors acknowledge the National Key Research and Development Program (Grant No. 2016YFD0200602).

References

1. Fan, Z., Simone, G., Yuping, B., et al.: Estimation of wheat water status by reflectance measurements. Trans. CSAE **21**(S), 215–217 (2005)
2. Ji, H., Wang, P., Yan, T.: Estimations of chlorophyll and water contents in live leaf of winter wheat with reflectance spectroscopy. Spectrosc. Spectr. Anal. **27**(3), 514–516 (2007)
3. Li, F., Zhao, C., Wang, J., et al.: Diagnosis of nitrogen nutrition of flue-cured tobacco with chlorophyll meter. Plant Nutr. Fertil. Sci. **13**(1), 136–142 (2007)
4. Wang, D., Ji, J., Gao, H.: The effect of MSC spectral pretreatment regions on near infrared spectroscopy calibration results. Spectrosc. Spectr. Anal. **34**(9), 2387–2390 (2014)
5. Yu, D., Cheng, W., Wang, Q., et al.: Construction of analysis model of rice seed components based on near infrared reflectance spectroscopy. J. Light. Scatt. **27**(4), 384–389 (2015)
6. Li, L., Huang, H., Zhao, S., et al.: NIR spectra detection model of protein, fat, total sugar and moisture in rice. J. Chin. Cereals Oils Assoc. **32**(7), 121–126 (2017)
7. Cao, H., Li, D., Liu, L., et al.: Near infrared spectroscopy quantitative analysis model based on incremental neural network with partial least squares. Spectrosc. Spectr. Anal. **34**(10), 2799–2803 (2014)
8. Lai, L., Ma, W., Chen, H.: Wheat protein nondestructive analysis with near infrared reflectance spectroscopy combined with artificial neutral networks. J. China Univ. Metrol. **26**(1), 55–59 (2015)

9. Kuang, J., Guan, X., Liu, J.: Rapid determination of protein and fat contents in raw milk by near infrared spectroscopy analysis. J. Anal. Sci. **31**(6), 783–786 (2015)
10. Zheng, W., Ming, J., Yang, M., et al.: Hyperspectral estimation of rice pigment content based on band depth analysis and BP neural network. Chin. J. Eco-Agric. **25**(8), 1224–1235 (2017)
11. Yao, X., Wang, X., Huang, Y., et al.: Estimation of sugar to nitrogen ratio in wheat leaves with near infrared spectrometry. Chin. J. Appl. Ecol. **26**(8), 2371–2378 (2015)